JPET Fast Forward. Published on February 10, 2009 as DOI: 10.1124/jpet.108.147496

JPET #147496

Potent *in vivo* anti-angiogenic effects of GS-101, an antisense oligonucleotide preventing the expression of Insulin Receptor Substrate-1

Salman Al-Mahmood, Sylvie Colin, Nada Farhat, Eric Thorin, Céline Steverlynck, Sylvain Chemtob

Gene Signal Laboratories, Genopole, 4 Rue Pierre Fontaine, 91000 Evry, France (SAM, SC, CS) ; Centre de Recherche de l'Institut de Cardiologie de Montréal, Montréal, Québec H1T 1C8, Canada (NF, ET); Université de Montréal, Faculty of medicine, Departments of Pediatrics, Ophthalmology, and Pharmacology, Research Center of Hôpital Sainte-Justine, Montréal, Québec H3T 1C5, Canada (SC).

JPET #147496

RUNNING TITLE PAGE

a) Running title : Anti-angiogenic effects of the antisense GS-101 *in vivo*

b) Address correspondence to: Dr. Salman Al-Mahmood, Gene Signal Laboratories, 4 Rue Pierre Fontaine, 91000 Evry, France. Tel: +33 (0)145404363; Fax: +33 (0)160878949 ; Email: sam@genesignal.com

c) Text pages: 26

Tables: 0

Figures: 7

References: 34

Abstract: 211

Introduction: 457

Discussion: 826

d) Abbreviations: FGF_2, fibroblast growth factor-2; hEC human endothelial cells; IGF, insulin-like growth factor; IL-1β, interleukin-1β; IRS-1, insulin receptor substrate-1; PBS, physiological buffer solution; mAb, monoclonal antibody; RT-PCR, reverse transcriptase polymerase chain reaction; VEGF-A, vascular endothelial growth factor-A.

e) Recommended section: Cardiovascular

Abstract

Angiogenesis is a complex phenomenon regulated by both pro- and anti-angiogenic factors such as the vascular endothelial growth factor (VEGF), and inflammation may be involved in the process. Although antagonizing VEGF has been proposed as a therapeutic approach to limit corneal angiogenesis, alternative targets are needed. In this study, we demonstrate that, under pro-angiogenic experimental conditions, human endothelial cells (hEC) express more insulin receptor substrate-1 (IRS-1) proteins relative to quiescent cells. The antisense oligonucleotide GS-101 targeting IRS-1 mRNA, dose-dependently inhibited ($P<0.01$) both IRS-1 expression and *in vitro* angiogenesis (hEC tube-like structure formation) with IC_{50} of 8.51±3.01 μM (mean±sem) and 2.47±0.56 μM, respectively, demonstrating that partial IRS-1 down-regulation interferes with angiogenesis. The anti-angiogenic effects of GS-101 were associated with a decrease in protein kinase B (Akt) activation but not mitogen-activated protein kinase-1/2, and a dose-dependent reduction in VEGF-A (IC_{50}=5.59±2.76 μM) and the pro-inflammatory cytokine lL-1β (IC_{50}=2.19±1.07 μM) mRNA expression. Accordingly, once daily topical application of GS-101 dose-dependently inhibited injury-dependent corneal angiogenesis *in vivo* ($P<0.05$). GS-101 *in vivo* efficacy was achieved at final tissue concentrations within *in vitro* EC_{50} for IRS-1 down-regulation. In conclusion, these results suggest that IRS-1 is important for angiogenesis and that GS-101, by inhibiting angiogenesis, could become a novel therapeutic tool against corneal angiogenesis.

Introduction

Angiogenesis is the formation of new blood vessels from pre-existing capillaries. It is necessary for normal tissue growth and repair. Lack of angiogenesis following ischemia for example, leads to heart failure (Carmeliet et al., 1999). Conversely, in several diseases, excessive angiogenesis contribute to the pathological process which could benefit from its therapeutic inhibition (Hanahan and Folkman, 1996). Insulin receptor substrate-1 (IRS-1) is a cytoplasmic docking protein downstream of activated cell surface receptors, including insulin, insulin-like growth factor (IGF), prolactin, growth hormone, VEGF-A receptors, and selected cytokine receptors (Hanahan and Folkman, 1996; White, 1998; Liang et al., 1999; Shaw, 2001; Senthil et al., 2002). The IRS-1 protein is recruited to receptors through pleckstrin homology and phospho-tyrosine-binding domains in its N-terminal, and mediates its functions by organizing signaling complexes at sites of receptor activation (White, 1998). Upon its phosphorylation on tyrosine residues in their C termini, IRS-1 recruit downstream SH2-proteins to initiate intracellular signaling cascades (White, 1998). Although IRS-1 is highly homologous to other insulin receptor substrates (IRS-2, IRS-3, and IRS-4), there is evidence for unique functions for each of the four IRS family members. IRS-$1^{-/-}$ mice have a 50% reduction in intrauterine growth, impaired glucose tolerance, and a decrease in insulin/IGF-1-stimulated glucose uptake *in vivo* and *in vitro*. However, these mice do not develop diabetes, because they maintain normal numbers of pancreatic β-cells, likely due to a compensatory recruitment of a related protein, IRS-2 (Araki et al., 1994). IRS-$2^{-/-}$ mice are of normal size at birth but exhibit brain defects and develop early-onset diabetes due to a combination of peripheral insulin resistance and β-cell failure (Withers et al., 1999; Schubert et al., 2003). IRS-$3^{-/-}$ mice are phenotypically normal, while IRS-$4^{-/-}$ mice have mild reproductive and insulin sensitivity defects (Liu et al., 1999; Fantin et al., 2000).

The role of IRS-1 in angiogenesis stems from the demonstration that insulin and IGF systems have been implicated in several vascular diseases, including angiogenesis (Delafontaine et al., 2004). IRS-1 could mediate the regulation of VEGF (Miele et al., 2000) or other pro-angiogenic cytokines such as IL-1β (White, 1998; Sainson et al., 2008) as well as by interactions with integrins. Insulin increases the expression of VEGF in retinal pigment epithelial cells (Slomiany and Rosenzweig, 2004), and VEGF type-2 receptor recruits IRS-1 upon its activation (Senthil et al., 2002). In the neonatal mouse model of hypoxia-induced retinal angiogenesis, the growth of pathologic vessels was reduced in IRS-1$^{-/-}$ mice, suggesting that IRS-1 plays an important role in the development of retinal neovessels (Jiang et al., 2003). We therefore studied the pathways by which IRS-1 contributes to neovessel formation using a newly developed antisense oligonucleotide, GS-101 (patents US#7,417,033; EP#1,409,672; CA#2,451,874), that reduces IRS-1 mRNA and protein expression.

Methods

Animals. The procedures and protocols have been reviewed to comply with the humane use of animals and approved by the Animal Ethical Committee of the Ste-Justine Hospital Research Center in conformity with the *Association for Research in Vision and Ophthalmology's statement (ARVO) on the Use of Animals in Ophthalmic Research*, and the *Guide for the Care and Use of Laboratory Animals* of Canada (Protocol number S04-37). Eighty-eight, 5-week old male Lewis rats and 20 pups from CD1 dams were used (Charles River Laboratories, Quebec, Canada).

GS-101. GS-101 is a 25mer phosphorothioate with a molecular weight of 8,036 Da of the following sequence :

5'-TATCCGGAGGGCTCGCCATGCTGCT-3'

GS-101 is stable in sterile saline solution (0.9% NaCl) for up to 3 months at room temperature and was used as such. Good manufactory practice (GMP) batches of GS-101 were provided by the company Gene Signal (patents US#7,417,033; EP#1,409,672; CA#2,451,874). The scramble oligonucleotide used in this study was of the following sequence:

5'-TGGACCTCTGGAGCTCTCGACGTGC-3'

Angiogenesis-related gene identification. The *in vitro* angiogenesis assay and the identification of angiogenesis-related genes were carried out according to the published US Patent #6,716,585 and European Patent #EP1,566,387, with slight modifications. Differential display and *in vitro* angiogenesis assay (endothelial cell capillary tube-like structures) experiments were performed in human umbilical vein endothelial cells (Jaffe et al., 1973), while all other experiments were performed in human microvascular endothelial cells (Cambex, Emerainville, France). Human endothelial cells (hEC) were cultured in complete EGM2-MV medium (Lonza, Levallois-Perret,

France), seeded onto type-1 collagen (BD Biosciences, le Pont de Claix) layer. They were cultured either in EGM2-MV (Lonza) medium alone or supplemented with 40 ng/ml of FGF_2 (Invitrogen, Oxon, UK). In these experimental conditions, tube-like structure develops on top of the confluent endothelial cell layer (Fig. 1A), which contrasts with more common endothelial cell-based tube-like structure developing on Matrigel (Fig. 2C). At maximal capillary tube-like formation, *i.e.* after 24h, cells were quickly washed with PBS at room temperature and directly re-suspended in the lysis buffer of the RNA extraction kit NucleoSpin RNA II kit; Macherey-Nagel, Hoerdt, France). Total RNA (2 μg) from each condition was subjected to reverse transcription with oligodT (0.1 µM), deoxynucleoside triphosphates (dNTPs, 0.5 mM, MBI Fermentas, St. Rémy Les Chevreuse, France), and Superscript II reverse transcriptase (Invitrogen), in a total reaction volume of 11 μl, at 65°C for 5 min. This cycle was followed by a second by mixing 4 µL 5x first-strand buffer, 2 µl 0.1M DTT and 1 µl RT Superscript II (Invitrogen) reverse transcriptase followed by 2 successive incubations steps of the mixture: 1) 42°C for 1h; 2) 72°C for 15min. The synthesized cDNA was used immediately for differential display analysis of gene expression using [α^{33}P]dCTP and Delta Differential Display Kit (Clontech). The PCR products were then resolved in SDS-PAGE, 6% acrylamid, and the gel slab was drayed, autoradiographed, and the part of the gel slab corresponding to the cDNA of interest was cut. The cDNA of interest was recovered from the gel, inserted in PGEM Easy vector (Promega) and amplified in *E. coli*, extracted, purified, and sequenced to identify the cDNA of interest.

Real-time reverse transcription–polymerase chain reaction assay. After exposure to various concentrations of GS-101 (0-20 µM) or vehicle for 24 h, hEC (5×10^5 cells/ ml), total mRNA

were isolated using NucleoSpin RNA II kit. RNA yields and purity were assessed by spectrophotometric analysis. The real-time RT-PCR was performed as previously described (Voghel et al., 2008). Briefly, 0.5 μg total RNA was reverse transcriped with random hexamer primers and M-MLV (200 U, Invirogen), and the synthesized cDNA was used immediately for real-time PCR amplification using the DNA-binding dye SYBR Green I for the detection of PCR products and the following primers: for VEGF-A (sense, 5′-GAGGGCAGAATCATCACGAA-3′; antisense, 5′-TGCTGTCTTGGGTGCATTGG-3′); for IL-1β (sense, 5'-AATCTCCGACCACCACTACA-3'; antisense, 5'-TGATCGTACAGGTGCATCGT-3'); for GAPDH (sense, 5′- TGAAGGTCGGAGTCAACGGA-3′; antisense 5′-CATTGATGACAAGCTTCCCG-3′). The real-time PCR reactions were carried out with the DNA Engine OPTICON 2 continuous fluorescence detector (MJ Research, Waltham, MA, U.S.A.). The results were quantifyed using the equation: $Copy_{TF}$:$Copy_{GAPDH}$= $2C(t)_{GAPDH} - C(t)_{TF}$. All PCR products were analyzed by electrophoresis on a 1.5% agarose gel, visualized with ethidium bromide, and analyzed using the Genesnap 6.00.26 software (Syngene, Cambridge, U.K.). Densitometric analysis was performed using GeneTools Analysis Software Version 3.02.00 (Syngene).

***In vitro* angiogenesis assays and quantification.** The formation of capillary tube-like structures was assessed on a solubilized Matrigel (Grant et al., 1989). Ninty-six well black plates with lids (PerkinElmer) were coated with Matrigel, and the hEC were seeded on the polymerized matrix at a density of 1.2×10^4 cells/well. When tested, GS-101, scramble GS-101 oligonucleotide, or triciribine (Akt inhibitor)(Shein et al., 2007) was present in the medium during the incubation. After 18±1h at 37°C in 5% CO_2, cells were labeled with Calcein and images were acquired using

JPET Fast Forward. Published on February 10, 2009 as DOI: 10.1124/jpet.108.147496
This article has not been copyedited and formatted. The final version may differ from this version.

Olympus fluorescence microscope equipped with, FITC-filter λ_{ex}: 470-490 nm - λ_{em} 517. The degree of tube formation was quantified by measuring the area occupied by the tubes in each well using the National Institute of Health Image J Software. Data collected were used to calculate IC_{50} values, using software GraphPad Prism 5, using a nonlinear regression of "log (inhibitor) *vs.* variable slope". Y=Bottom + (Top-Bottom)/(1+10^((LogIC_{50}-X)*Hill Slope)). Mean of IC_{50} of n replicates in intra-assay and inter-assay was calculated, standard deviation and CV % were determined.

Protein quantification. Serum-deprived hEC were incubated with different concentrations of GS-101, scramble GS-101 oligonucleotide, VEGF or FGF_2 at 37°C under 5% CO_2 for 6 h. After 3 washes with ice-cold PBS, cells were suspended with the protein extraction buffer (PEB) (20 mM Tris-HCl pH 7.5, 150 mM NaCl, 1 mM EDTA, 1 mM EGTA, 1% Triton, 25 mM sodium pyrophosphate, 1 mM β-glycero-phosphate, 1 mM Na_3Vo_4, 1 µg/ml leupeptine, 1 µM PMSF). The protein content was measured by Bradford. IRS-1 concentration in the extracts was determined by Path-Scan Total IRS-1 Sandwich ELISA kit (Cell Signaling technology) according to the manufacturer's instructions. The data were collected from 4 separates experiments performed in duplicate and expressed relative to control cells (vehicle). IC_{50} values were calculated using GraphPad Prism 5, using a nonlinear regression of "log (inhibitor) *vs.* variable slope". Y=Bottom + (Top-Bottom)/(1+10^((LogIC_{50}-X)*Hill Slope)).

To confirm the results obtained with Path-Scan Total IRS-1 Sandwich ELISA kit, equal volumes of the adjusted cells extracts were also resolved by SDS-PAGE, followed by the transfer of proteins to PVDF membrane. The membrane was incubated with 5% defatted milk solution in BPS-Tween 0.5% for 1 h, followed by two washes, and immunoblotting with either an anti-IRS-

1-HRP conjugate (1/300 dilution; Santa cruz), anti-GAPDH-HRP conjugate (Santa cruz), mouse anti-p-Erk1/2 (Santa Cruz, ref sc-7383), anti-p-Akt (1/200 dilution, Ser473, ref sc-7985-R; Santa Cruz), and anti-goat-HRP conjugate (1/250 dilution, Santa Cruz). Rabbit polyclonal VEGF (147; ref: sc-507, Santa-Cruz) and goat polyclonal IL-1β (C-20; ref : sc-1250, Santa-Cruz), anti-IRS-2 (Santa Cruz, sc-8299, 1/200; anti-rabbit Santa Cruz sc-2305, 1/30 000) and anti-IRS-4 (Santa Cruz, sc-100854, 1/200; anti-mouse, Santa cruz sc-2302, 1/30 000). Proteins were then monitored by ECLplus (GE Healthcare).

Mouse Model of Corneal Neovascularization. Only the right eye of each mouse was used. Neovascularization was induced by mechanical resection of the corneal epithelium debridement, using a method described by Amano et al. (Amano et al., 1998) and previously used in our group (Mwaikambo et al., 2006). Animals (approximately 8 weeks old) were anesthetized before all surgical procedures with isoflurane (Abbott, Montréal, Québec, Canada). Topical proparacaine (Alcon Canada, Mississauga, Ontario) and 2 µL of 0.15 M NaOH were applied to the central cornea of each mouse. The corneal and limbal epithelia were then removed by scraping. The eye was then washed extensively with saline followed by application of erythromycin ophthalmic ointment. Eyelids were subsequently sutured with 6.0 silk threads and buprenorphine (0.05 mg/kg) was administered postoperatively. On Day 3 after surgery, the animals were randomly assigned to the respective treatment groups: 0.9 % NaCl (sterile vehicle prepared daily; n=11); 100 µM (n=6), 200 µM (n=9), 400 µM (n=9), or 800 µM (n=9) GS-101 (Gene Signal; pH 6.8). The suture was then removed and the treatments initiated. A 30-µl volume of the control or test drug was administered topically once per day onto the wounded eye for 7 days, the last drop being given day 9 post-surgery. All experiments were performed day 10.

Labelling and Quantification of Corneal Neovascularization. On Day 10, under general anesthesia (O_2: 60%; isoflurane: level 2-3), the upper body was perfused with Fluorescein-Dextran 2 x 100 000 (Sigma-Aldrich) in order to fill the microvasculature. Animals were subsequently euthanized with a lethal dose of isoflurane. The eyes were then enucleated and fixed in 4% paraformaldehyde in PBS 1X for 3 h and thereafter washed extensively (3 times 10 min) in PBS 1X. The cornea including 1 mm-limbus was dissected free of the eye under the dissecting microscope and then flattened on a glass slide by radial incisions and using Gelmount anti-fading agent. Corneas were observed using a Nikon eclipse E800 fluorescent microscope and images captured with a Nikon digital camera DXM 1200 using Nikon ACT 1 version 2.62 software. The images were then compiled, analyzed, and quantified using Adobe Photoshop 7.0 image analysis software. The ratio [(neovascularized area/total cornea area) x 100] was used to provide a measure of the percent vascularized cornea.

Statistical analysis of the data. Continuous data are presented as mean±sem, with n indicating the number of assays performed on independent cultures. Appropriate univariate analysis (t-test or ANOVA with Fisher's post hoc test) was used (Statview 4.5). A $p<0.05$ was considered statistically significant.

Results

IRS-1 expression is up regulated under angiogenic conditions. Twenty-four hours exposure of hEC to FGF_2 led to differentiated capillary tube-like structures (Fig. 1A). Differential gene expression profiling revealed profound differences, as expected. Among the changes, we found that IRS-1 expression increased both at the mRNA (Fig. 1B) and protein (Fig. 1C) level in differentiated cells. In addition to the increased expression, the level of tyrosine phosphorylation of IRS-1, a marker of activation (White, 2002), was augmented in hEC undergoing capillary tube-like structure differentiation (Fig. 1E,F). In the absence of FGF_2, the rate of cellular proliferation (-14±5% at confluence of untreated cells) was not significantly altered in the presence of GS-101 (10 μM; data not shown).

In addition to FGF_2, VEGF increased IRS-1 expression (Fig. 1G). Both angiogenic factors, however, neither increased the expression of IRS-2 or IRS-4 proteins (Fig. 2H,I).

GS-101 inhibits IRS-1 expression and *in vitro* capillary tube-like structure formation in a dose-dependant manner. To validate the possible involvement of IRS-1 in the intracellular cascade of events that leads to *in vitro* angiogenesis, differentiated hEC grown in Matrigel were exposed to increasing concentrations of GS-101. In contrast to the scramble oligonucleotide form of GS-101 (Sc-GS-101), GS-101 prevented IRS-1 expression (Fig. 2A,B) with an IC_{50} = 8.51±3.01 μM; this reduction in IRS-1 expression was paralleled with the concentration-dependent (IC_{50} = 2.47±0.56 μM) reduction in capillary tube-like structure formation (Fig. 2C,D).

Effects of GS-101 on Akt, ERK1/2 activation, and VEGF-A and IL-1β mRNA expression. We first investigated the influence of GS-101 on Akt and ERK1/2 activation. Following 4 hours

JPET Fast Forward. Published on February 10, 2009 as DOI: 10.1124/jpet.108.147496
This article has not been copyedited and formatted. The final version may differ from this version.

of incubation with GS-101, no changes in ERK1/2 activity were detectable (Fig. 3A). In contrast, GS-101 strongly decreased Akt activation (Fig. 3B). Accordingly, the Akt inhibitor triciribine induced a concentration-dependent inhibition of capillary tube-like structure formation (Fig. 3D,E).

We quantified the mRNA and protein expression levels of both VEGF-A and IL-1β in hEC. Following 6 hours of incubation with GS-101, both VEGF-A (Fig. 4A) and IL-1β (Fig. 4B) transcripts were reduced in hEC as measured by quantitative real time RT-PCR, which was paralleled by a reduction in protein expression (Fig. 4C). These inhibitory effects of GS-101 on mRNA expression occurred with IC_{50} of 5.59±2.76 μM (n=4) and 2.19±1.07 μM (n=4), for VEGF-A and IL-1β, respectively.

Effects of VEGF on GS-101 antiangiogenic activity. Exogenous addition of VEGF to hEC grown on Matrigel antagonized the anti-angiogenic effect of a low (2.5 μM) but not high (5 μM) concentration of GS-101 (Fig. 5).

Inhibition of corneal neovascularization by topical application GS-101. Before initiation of treatment at day 3 post-surgery, all eyes had developed a circular neovascularization of the corneas, with new vessels progressing from the limbus 360° toward the center of the cornea. At day 10, confocal microscopy of dextran-FITC–labeled corneal flatmounts illustrates the reduced thickness of persisting neovessels in GS-101-treated rats compared to corneas isolated from untreated animals (Fig. 6A). In the non-treated rats, neovascularization covered 54±4% (n=11) of the cornea. Eye-drop application of GS-101 once daily limited ($P<0.05$) corneal neovascularization in a dose-dependent manner (Fig. 6B). While the lowest concentration of 100

µM had no effect on angiogenesis, inhibition of its progression started at 200 µM (≈15%), to increase at 400 µM (≈34%) and plateau at 800 µM (≈38%). No toxic effect or local irritation due to the topical application of GS-101 was observed.

Correlation of the *in vitro* and the *in vivo* concentrations of GS-101. Ninety min following a single topical application of ^{35}S-labeled GS101 (36.36 µg in 10 µl, from a stock solution of 450 µM) on the cornea of a rabbit eye, quantification of the radioactivity by liquid scintillation revealed that an average of 0.025% of the applied amount of GS-101 (*i.e.* 9.1 ng) remained in the cornea (Fig. 7). Estimation of the volume of the cornea, based on published data (vertical diameter: 11 mm, horizontal: 11.7 mm, central thickness: 0.5 mm and 1 mm peripherally; www.EYEWEB.org, under intraocular anatomy), gives an approximate corneal volume of 64.35 mm^3 (*i.e.* 64.35 µl). The corneal concentration of GS-101 can be estimated to be 17.4 nM (i.e. 139.86 ng/ml or 139.86 µg/l). A cornea area was selected randomly and magnified 3 times (Fig. 7B) to analyze radioactivity: the signal density in the endothelial layer fitted best to standard n°9 (^{35}S-labeled GS-101, 3,619 dpm/mg). In contrast, the radioactivity of other corneal tissues, including the stroma and epithelium, corresponded better to standard n°6 (45 dpm/mg), indicating that the relative concentration of GS-101 in the endothelial layer is 80.4 times higher than in the corneal stroma. By combining the measure of the concentration of GS-101 in the cornea by liquid scintillation (i.e. 17.4 nM), and the radioluminogram-based relative concentration, the concentration of GS-101 in the endothelial layer of the cornea can be estimated to 1.4 µM.

JPET Fast Forward. Published on February 10, 2009 as DOI: 10.1124/jpet.108.147496
This article has not been copyedited and formatted. The final version may differ from this version.

Discussion

In this study, we demonstrate that IRS-1 expression is up-regulated in hEC undergoing capillary tube-like structure formation (*in vitro* angiogenesis). Conversely, we demonstrate that partial inhibition of IRS-1 expression by GS-101, an antisense oligonucleotide against IRS-1, inhibits *in vitro* and *in vivo* angiogenesis. This validates the concept that IRS-1 is directly involved in the angiogenic process, whether it is induced by a growth factors or likely corneal injury.

The involvement of IRS-1 in the angiogenic process has been suggested by the demonstration that hyperoxia-induced retinal angiogenesis was reduced in IRS-$1^{-/-}$ mice (Jiang et al., 2003). Our data extend these findings by demonstrating for the first time that not only the expression of IRS-1 increases (but not that of IRS-2 and IRS-4), but also its activation, as shown by the increased amount of phosphorylated IRS-1 protein. It is known that IRS-1 phosphorylation contributes to the activation of two distinct but complementary down-stream signaling pathways, *i.e.* the PI_3-kinase/Akt and Ras/MAP kinase pathways, both interacting with the VEGF pathway (White, 2002). In our hands, GS-101 only decreased Akt activity (Shaw, 2001), without affecting ERK1/2, suggesting that the IRS-1 pathway is highly compartimentalized in hEC. Accordingly, triciribine reduced capillary tube-like structure formation in a concentration-dependent manner, without preventing it, as in the retina of IRS-$1^{-/-}$ mice (Jiang et al., 2003) or in the presence of GS-101 both *in vitro* and *in vivo*.

VEGF has been reported to increase ERK1/2 activity (Bullard et al., 2003). The decrease in VEGF-A expression, also reported in IRS-$1^{-/-}$ mice (Jiang et al., 2003), suggests that in our experimental conditions ERK1/2 neither regulates VEGF transcription nor *in vitro* angiogenesis. Our data rather point to a prominent role of Akt in the angiogenic pathway. Surprisingly, however, while GS-101 induced a concentration-dependent inhibition of IRS-1 expression, a

complete inhibition of hEC capillary tube-like structure formation *in vitro* was achieved at a concentration of GS-101 (5 μM) that reduced IRS-1 and VEGF-A expression by only 40%. Although the reduction in VEGF-A expression is consistent with previously published data (Jiang et al., 2003), it shows that only a partial inhibition of IRS-1 expression is necessary to prevent *in vitro* angiogenesis. This is confirmed *in vivo*, where a daily single eye drop of GS-101 (400 μM), leading to a concentration of ≈1.4 μM within the endothelial layer of the cornea, is sufficient to inhibit corneal angiogenesis, as previously reported (Andrieu-Soler et al., 2005), with however, no additional benefit of a higher concentration, explaining the lack of further prevention of angiogenesis in IRS-$1^{-/-}$ mice (Jiang et al., 2003). A limitation in these estimates is our lack of kinetic data following repeated treatment, as it is possible that GS-101 accumulates in the cornea. Nonetheless, our data suggests that an incomplete reduction in IRS-1 expression limits angiogenesis, both *in vitro* and *in vivo*, confirming a previous report (Andrieu-Soler et al., 2005). Further, the partial inhibition of *in vitro* angiogenesis by a low concentration of GS-101 (2.5 μM) could be overcome by the exogenous addition of VEGF. This is an important result demonstrating that the anti-angiogenic effect of GS-101 can be overcome by increasing the concentration of a growth factor.

In addition to limit VEGF-A expression, GS-101 also reduced that IL-1β mRNA in a concentration-dependent manner. This latter result is in agreement with a previous report (Andrieu-Soler et al., 2005), and provides additional insight on the possible mechanism of action of IRS-1. In animal models of corneal neovascularization, VEGF, cytokines, and interleukins are known to be involved (BenEzra et al., 1990; Amano et al., 1998; Yamada et al., 2003). IL-1β is a potent pro-angiogenic factor in the cornea (BenEzra et al., 1990). This effect of GS-101 is well in phase with its anti-angiogenic activity, combining both a reduction in the activity of the VEGF

pathway and an anti-inflammatory action. Furthermore, these pharmacological effects of GS-101 are well within the predicted range of concentrations achieved *in vivo* in our experimental models.

These results prompted us to propose an alternative to direct anti-VEGF therapies (Bock et al., 2008a) by using GS-101 as a new tool to prevent corneal angiogenesis (Cursiefen et al., 2009) for patients in need of a therapeutic alternative to corneal grafting (Coster and Williams, 2003; Panda et al., 2007). The use of anti-VEGF therapies, although efficient, may not be devoid of side effects since VEGF has recently been proposed to be important for the maintenance and function of adult retina neuronal cells (Saint-Geniez et al., 2008). The reduction in IL-1β induced by GS-101 is a desired benefice in corneal neovascularization, in which inflammation is highly detrimental (Bock et al., 2008b).

In conclusion, our results demonstrate that GS-101, an antisense oligonucleotide targeting the expression of IRS-1, a scaffold protein known to regulate angiogenesis (White, 1998; Miele et al., 2000; Jiang et al., 2003), can limit *in vitro* and *in vivo* angiogenesis. Its topical application is safe and being tested in human (Cursiefen et al., 2009).

References

Amano S, Rohan R, Kuroki M, Tolentino M and Adamis AP (1998) Requirement for vascular endothelial growth factor in wound- and inflammation-related corneal neovascularization. *Invest Ophthalmol Vis Sci* **39**:18-22.

Andrieu-Soler C, Berdugo M, Doat M, Courtois Y, BenEzra D and Behar-Cohen F (2005) Downregulation of IRS-1 expression causes inhibition of corneal angiogenesis. *Invest Ophthalmol Vis Sci* **46**:4072-4078.

Araki E, Lipes MA, Patti ME, Bruning JC, Haag B, 3rd, Johnson RS and Kahn CR (1994) Alternative pathway of insulin signalling in mice with targeted disruption of the IRS-1 gene. *Nature* **372**:186-190.

BenEzra D, Hemo I and Maftzir G (1990) In vivo angiogenic activity of interleukins. *Arch Ophthalmol* **108**:573-576.

Bock F, Konig Y, Kruse F, Baier M and Cursiefen C (2008a) Bevacizumab (Avastin) eye drops inhibit corneal neovascularization. *Graefes Arch Clin Exp Ophthalmol* **246**:281-284.

Bock F, Onderka J, Dietrich T, Bachmann B, Pytowski B and Cursiefen C (2008b) Blockade of VEGFR3-signalling specifically inhibits lymphangiogenesis in inflammatory corneal neovascularisation. *Graefes Arch Clin Exp Ophthalmol* **246**:115-119.

Bullard LE, Qi X and Penn JS (2003) Role for extracellular signal-responsive kinase-1 and -2 in retinal angiogenesis. *Invest Ophthalmol Vis Sci* **44**:1722-1731.

Carmeliet P, Ng YS, Nuyens D, Theilmeier G, Brusselmans K, Cornelissen I, Ehler E, Kakkar VV, Stalmans I, Mattot V, Perriard JC, Dewerchin M, Flameng W, Nagy A, Lupu F, Moons L, Collen D, D'Amore PA and Shima DT (1999) Impaired myocardial angiogenesis and ischemic cardiomyopathy in mice lacking the vascular endothelial growth factor isoforms VEGF164 and VEGF188. *Nat Med* **5**:495-502.

Coster DJ and Williams KA (2003) Management of high-risk corneal grafts. *Eye* **17**:996-1002.

Cursiefen C, Bock F, Kruse FE, Borderie V, Wilhelm F, Schirra F, Seitz B, Meller D, Frueh Epstein B and Thiel M (2009) GS-101 eye drops, an antisense oligonucleotide against IRS-1, inhibit and regress corneal neovascularization: interim results of a multicentre double-blind randomized phase II clinical study. *Ophtamology* **in press**.

Delafontaine P, Song YH and Li Y (2004) Expression, regulation, and function of IGF-1, IGF-1R, and IGF-1 binding proteins in blood vessels. *Arterioscler Thromb Vasc Biol* **24**:435-444.

Fantin VR, Wang Q, Lienhard GE and Keller SR (2000) Mice lacking insulin receptor substrate 4 exhibit mild defects in growth, reproduction, and glucose homeostasis. *Am J Physiol Endocrinol Metab* **278**:E127-133.

Grant DS, Tashiro K, Segui-Real B, Yamada Y, Martin GR and Kleinman HK (1989) Two different laminin domains mediate the differentiation of human endothelial cells into capillary-like structures in vitro. *Cell* **58**:933-943.

Hanahan D and Folkman J (1996) Patterns and emerging mechanisms of the angiogenic switch during tumorigenesis. *Cell* **86**:353-364.

Jaffe EA, Nachman RL, Becker CG and Minick CR (1973) Culture of human endothelial cells derived from umbilical veins. Identification by morphologic and immunologic criteria. *J Clin Invest* **52**:2745-2756.

Jiang ZY, He Z, King BL, Kuroki T, Opland DM, Suzuma K, Suzuma I, Ueki K, Kulkarni RN, Kahn CR and King GL (2003) Characterization of multiple signaling pathways of insulin in the regulation of vascular endothelial growth factor expression in vascular cells and angiogenesis. *J Biol Chem* **278**:31964-31971.

Liang L, Zhou T, Jiang J, Pierce JH, Gustafson TA and Frank SJ (1999) Insulin receptor substrate-1 enhances growth hormone-induced proliferation. *Endocrinology* **140**:1972-1983.

Liu SC, Wang Q, Lienhard GE and Keller SR (1999) Insulin receptor substrate 3 is not essential for growth or glucose homeostasis. *J Biol Chem* **274**:18093-18099.

Miele C, Rochford JJ, Filippa N, Giorgetti-Peraldi S and Van Obberghen E (2000) Insulin and insulin-like growth factor-I induce vascular endothelial growth factor mRNA expression via different signaling pathways. *J Biol Chem* **275**:21695-21702.

Mwaikambo BR, Sennlaub F, Ong H, Chemtob S and Hardy P (2006) Activation of CD36 inhibits and induces regression of inflammatory corneal neovascularization. *Invest Ophthalmol Vis Sci* **47**:4356-4364.

Panda A, Vanathi M, Kumar A, Dash Y and Priya S (2007) Corneal graft rejection. *Surv Ophthalmol* **52**:375-396.

Sainson RC, Johnston DA, Chu HC, Holderfield MT, Nakatsu MN, Crampton SP, Davis J, Conn E and Hughes CC (2008) TNF primes endothelial cells for angiogenic sprouting by inducing a tip cell phenotype. *Blood* **111**:4997-5007.

Saint-Geniez M, Maharaj AS, Walshe TE, Tucker BA, Sekiyama E, Kurihara T, Darland DC, Young MJ and D'Amore PA (2008) Endogenous VEGF is required for visual function: evidence for a survival role on muller cells and photoreceptors. *PLoS ONE* **3**:e3554.

Schubert M, Brazil DP, Burks DJ, Kushner JA, Ye J, Flint CL, Farhang-Fallah J, Dikkes P, Warot XM, Rio C, Corfas G and White MF (2003) Insulin receptor substrate-2 deficiency impairs brain growth and promotes tau phosphorylation. *J Neurosci* **23**:7084-7092.

Senthil D, Ghosh Choudhury G, Bhandari BK and Kasinath BS (2002) The type 2 vascular endothelial growth factor receptor recruits insulin receptor substrate-1 in its signalling pathway. *Biochem J* **368**:49-56.

Shaw LM (2001) Identification of insulin receptor substrate 1 (IRS-1) and IRS-2 as signaling intermediates in the alpha6beta4 integrin-dependent activation of phosphoinositide 3-OH kinase and promotion of invasion. *Mol Cell Biol* **21**:5082-5093.

Shein NA, Tsenter J, Alexandrovich AG, Horowitz M and Shohami E (2007) Akt phosphorylation is required for heat acclimation-induced neuroprotection. *J Neurochem* **103**:1523-1529.

Slomiany MG and Rosenzweig SA (2004) IGF-1-induced VEGF and IGFBP-3 secretion correlates with increased HIF-1 alpha expression and activity in retinal pigment epithelial cell line D407. *Invest Ophthalmol Vis Sci* **45**:2838-2847.

Voghel G, Thorin-Trescases N, Farhat N, Mamarbachi AM, Villeneuve L, Fortier A, Perrault LP, Carrier M and Thorin E (2008) Chronic treatment with N-acetyl-cystein delays cellular senescence in endothelial cells isolated from a subgroup of atherosclerotic patients. *Mech Ageing Dev* **129**:261-270.

White MF (1998) The IRS-signaling system: a network of docking proteins that mediate insulin and cytokine action. *Recent Prog Horm Res* **53**:119-138.

White MF (2002) IRS proteins and the common path to diabetes. *Am J Physiol Endocrinol Metab* **283**:E413-422.

Withers DJ, Burks DJ, Towery HH, Altamuro SL, Flint CL and White MF (1999) Irs-2 coordinates Igf-1 receptor-mediated beta-cell development and peripheral insulin signalling. *Nat Genet* **23**:32-40.

Yamada J, Dana MR, Sotozono C and Kinoshita S (2003) Local suppression of IL-1 by receptor antagonist in the rat model of corneal alkali injury. *Exp Eye Res* **76**:161-167.

Footnotes

This work was supported by Gene Signal Laboratories through an unrestricted educational grant.

Legends for figures

Figure 1: Increased expression and activation of IRS-1 in hEC undergoing FGF_2-dependent tube-like structure formation. A) Cells were seeded onto a type 1 collagen matrix and incubated in the absence (1) or in the presence (2) of FGF_2 for 24 h. B) mRNAs were extracted, cDNA produced using random primers and differential gene expression analyzed. C) Increased expression of IRS-1 protein in differentiated hEC following SDS-PAGE and Western blot. D) Membranes were then stripped and re-probe with anti-GAPDH mAb to confirm equal protein loading. E) Increased activation of IRS-1 protein by phosphorylation (as evidenced by IRS-1 protein-immunoprecipitation followed by anti-PY20 mAb blot), following equal amount of total IRS-1 protein loading (F). Effect of FGF_2 and VEGF on IRS-1, 2 and 4 expression (G,H,I,J) by hEC. Equivalent amounts of hEC proteins extracts were used to quantify IRS-1, 2 and 4 proteins by Western blot following SDS-PAGE.

Figure 2: Concentration-dependent inhibition of IRS-1 protein expression (A,B) and *in vitro* hEC tube-like structure formation on Matrigel (C,D) by GS-101. Equivalent amounts of hEC proteins extracts were used to quantify IRS-1 protein by ELISA Sandwich assay (A), and by Western blot following SDS-PAGE (B). The PVDF membranes were stripped and re-probe with anti-GAPDH mAb to control for equal loading (B). C) Representative images of hEC forming capillary tube-like structures in Matrigel and the concentration-dependent inhibitory effect of GS-101, and (D) summary of data expressed as mean±SD (n = 42) and reported *vs.* vehicle; as a control experiment, the scramble GS-101 oligonucleotide (Sc-GS-101, 10 µM) was used. *: $P < 0.01$ *versus* vehicle-treated group (0.9% NaCl).

Figure 3: Effects of 4hrs exposure to GS-101 (20 µM) on hEC p-ERK1/2 (A) and p-Akt (B) expression (measured by Western blot). Equal protein loading was controlled for by GAPDH immunoblotting (C). As a negative control, a scramble oligonucleotide of GS-101 was used (20 µM). (D) Representative images of hEC forming capillary tube-like structures in Matrigel and the concentration-dependent inhibitory effect of triciribine (Akt inhibitor). (E) Summary of data expressed as mean±SD (n = 3). *: $P < 0.01$ *versus* vehicle-treated control group (0 µM; 0.9% NaCl).

Figure 4: Effects of increasing concentration of GS-101 on the expression by hEC in Matrigel of VEGF-A mRNA (A) and IL-1β mRNA (B) measured by quantitative RT-PCR, and expressed as mean±SEM (n = 4). *: $P < 0.01$ *versus* vehicle-treated group (0.9% NaCl). (C) Representative Western blot analysis of VEGF-A and IL-1β protein production by hEC in Matrigel and increasing concentrations of GS-101. A scramble-GS-101 (Sc-GS-101) oligonucleotide was used as a negative control.

Figure 5: Impact of the addition of exogenous VEGF on GS-101-induced inhibition of capillary tube-like structure formation in Matrigel. Data are expressed as mean ± SEM (n=3). *: $P < 0.01$ *versus* vehicle-treated control group (0.9% NaCl); ‡: $P < 0.01$ *versus* 2.5 µM GS-101 alone.

Figure 6: Dose-dependent inhibition of *in vivo* inflammatory corneal angiogenesis by GS-101. The effect of GS-101 on corneal neovascularization at day 10 was monitored by fluorescent photographs of whole flatmounted corneas (A) and expressed as % of cornea area

neovascularization (B). Results are expressed as the mean±SEM. *: $P < 0.01$ *versus* vehicle-treated group (0.9% NaCl).

Figure 7: A) Representative radioluminogram of eye sections showing the bio-distribution and the relative concentration of ^{35}S-labeled GS-101 (36.36 µg) following a single eye drop at -90 min. B) Estimation of ^{35}S-labeled GS-101 tissue concentration using the blood calibration curve.

Figure 1

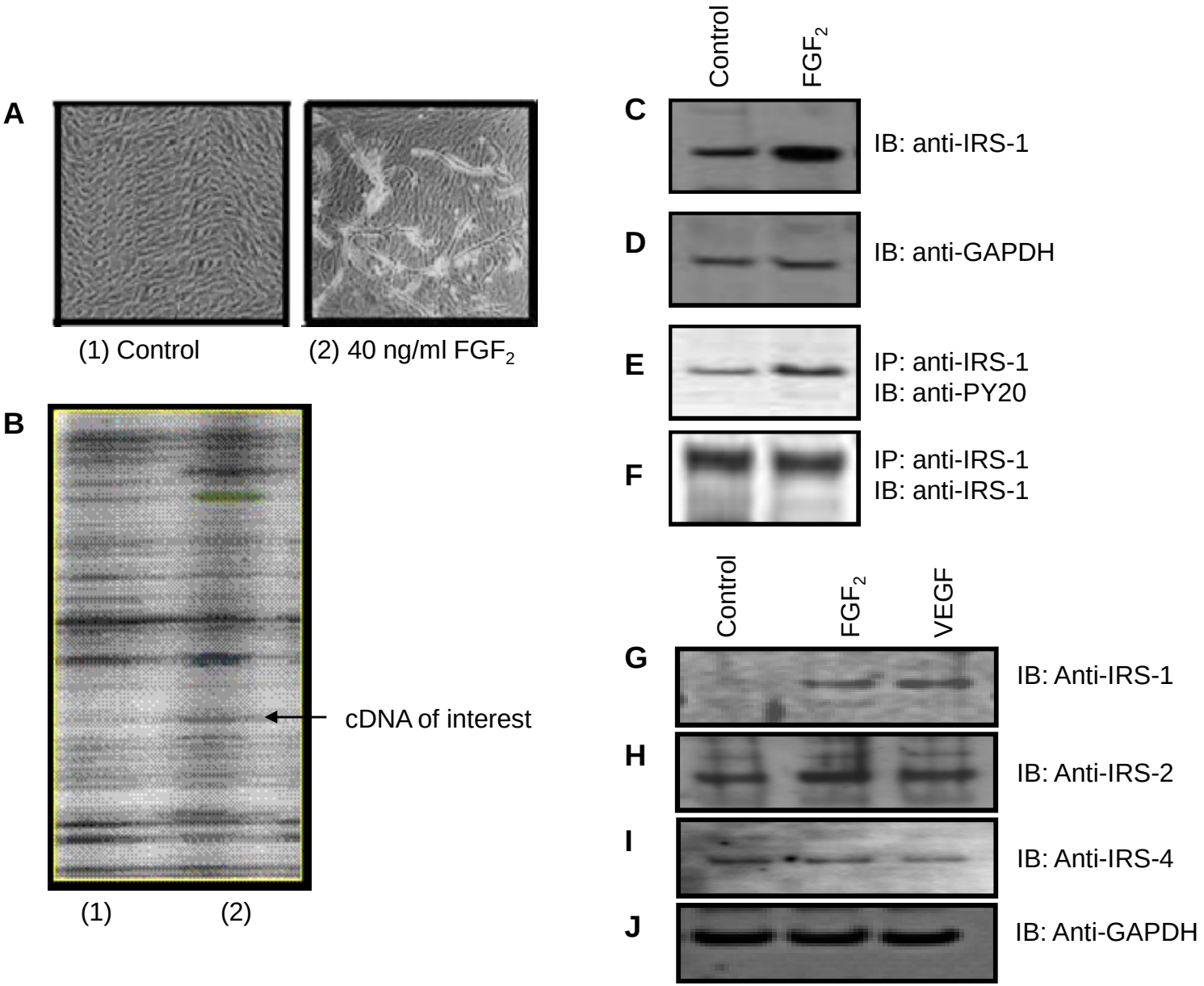

Figure 2

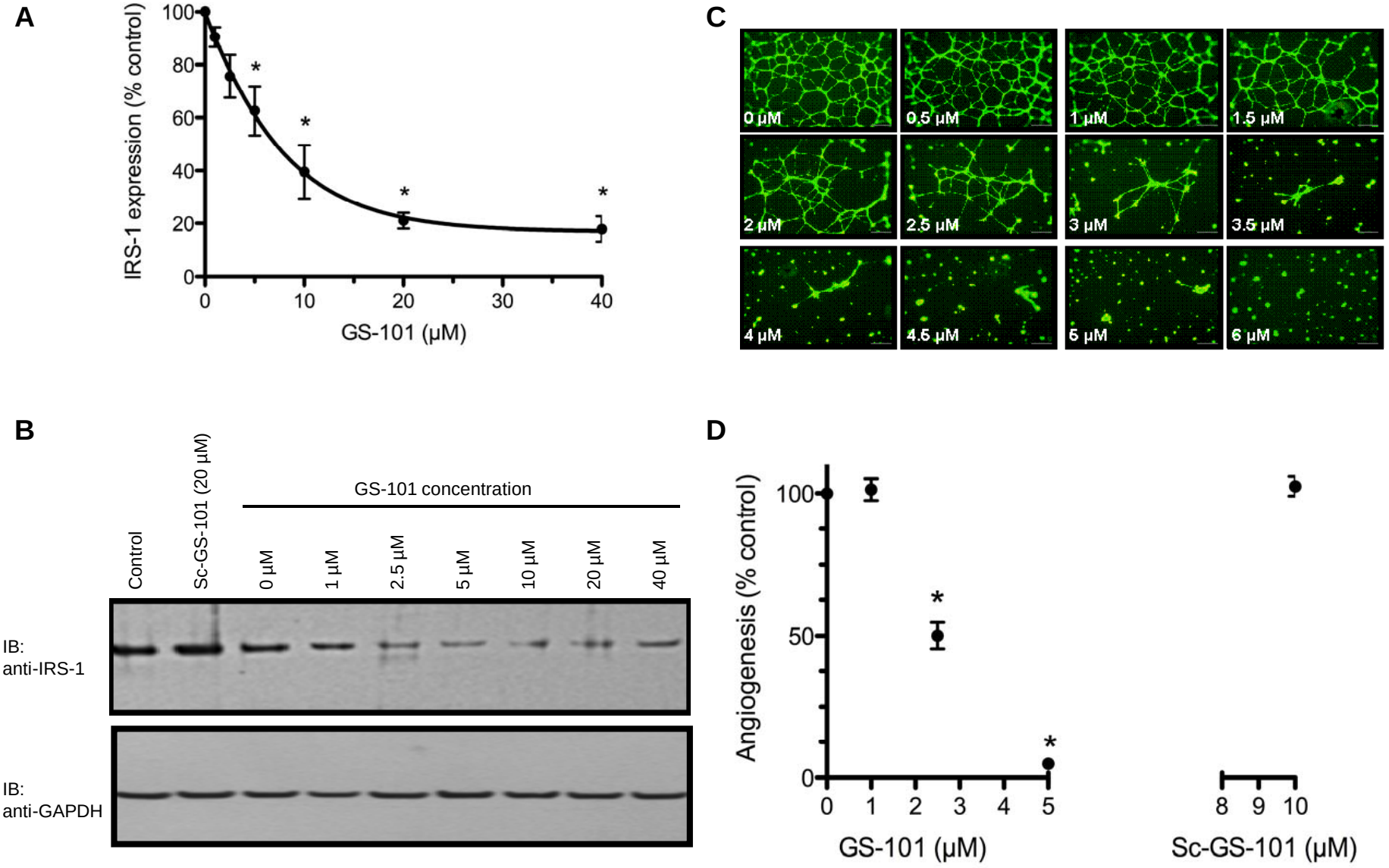

Figure 3

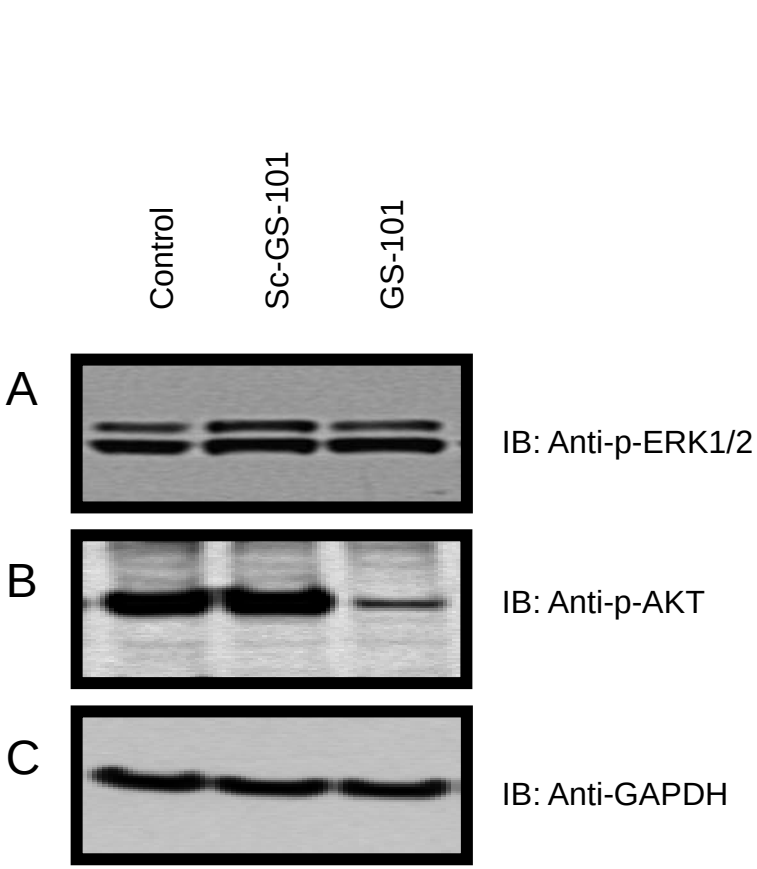

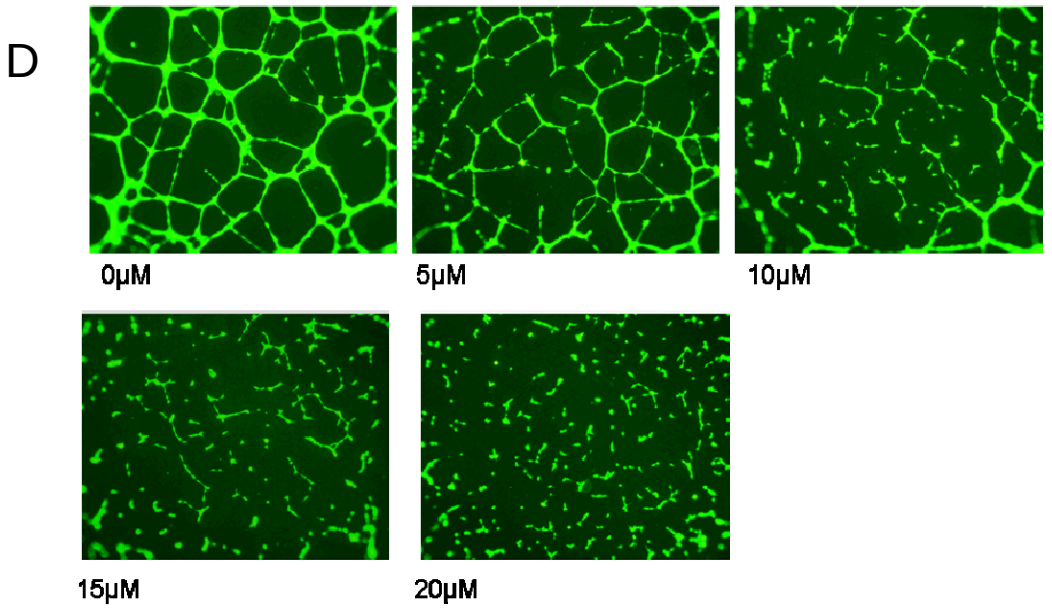

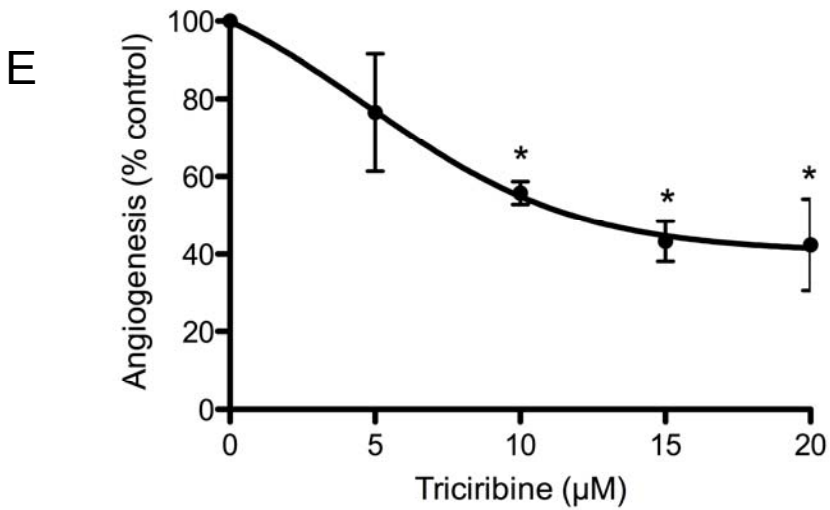

Figure 4

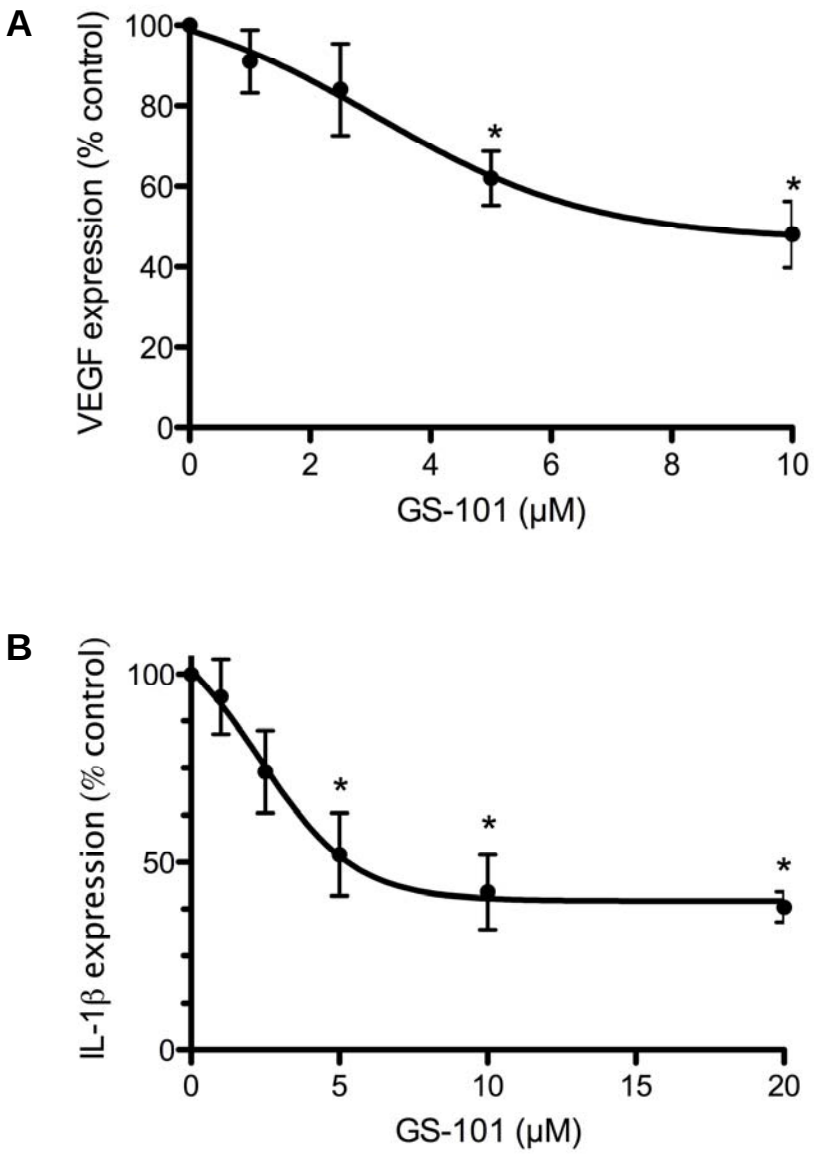

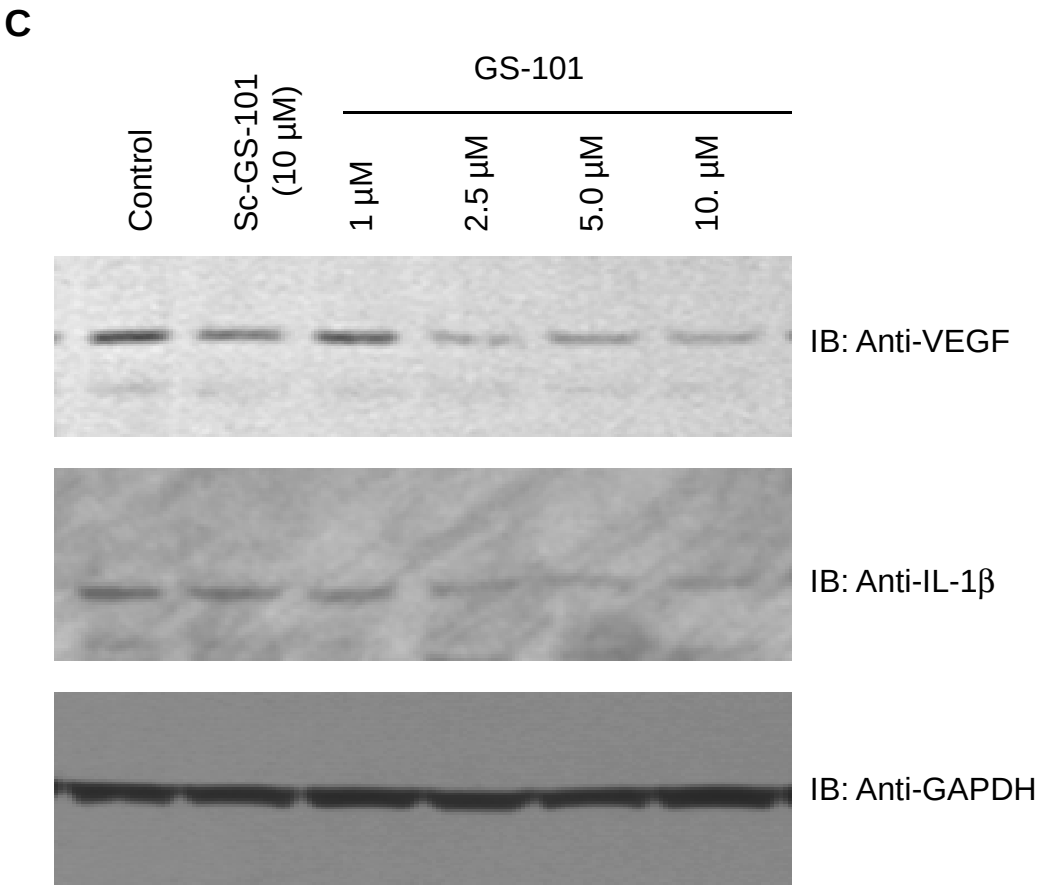

Figure 5

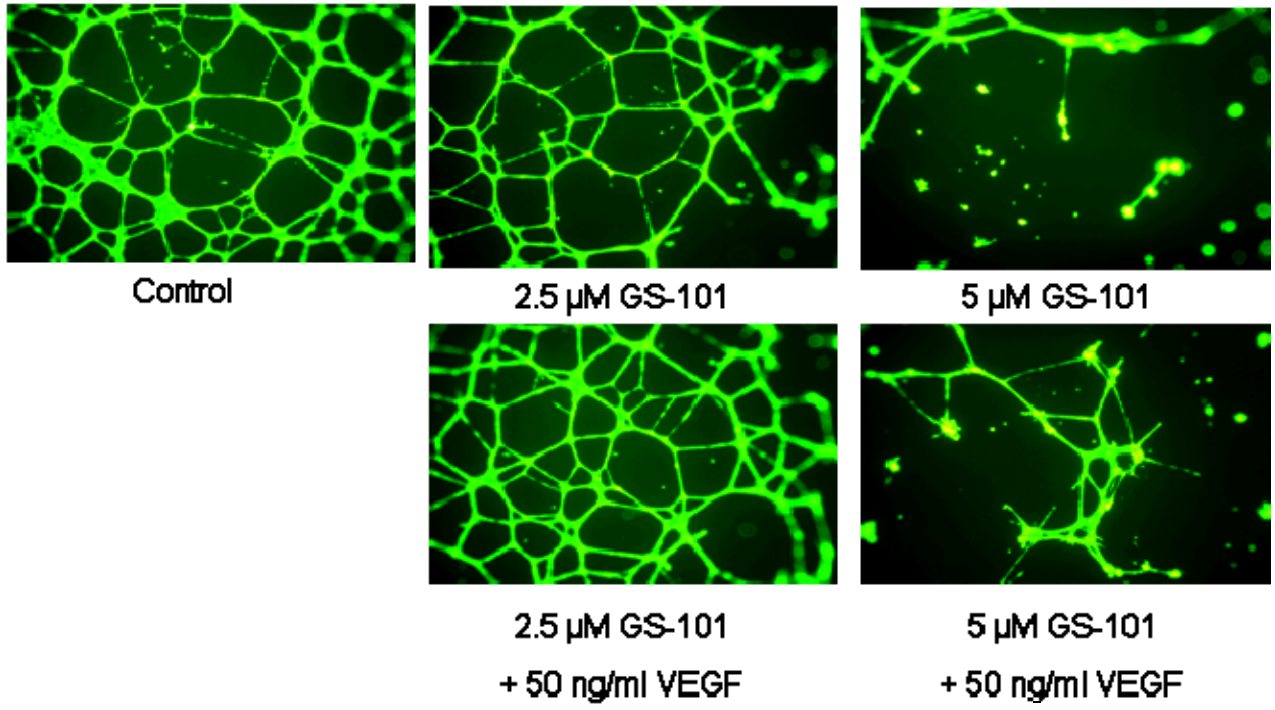

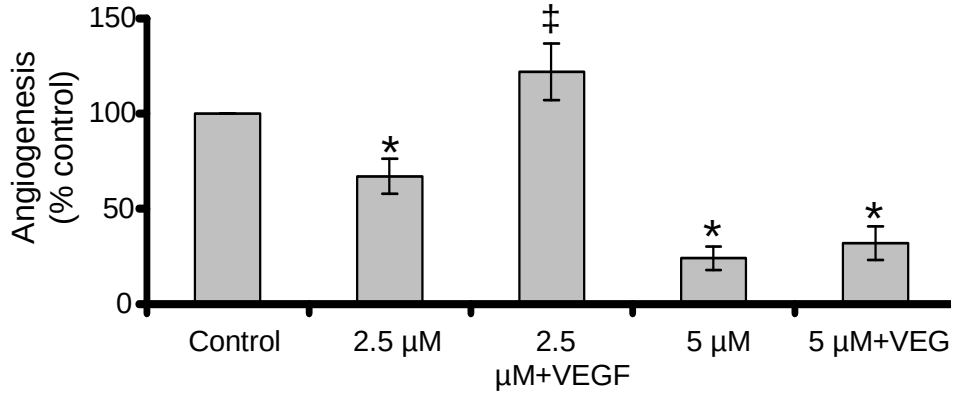

Figure 6

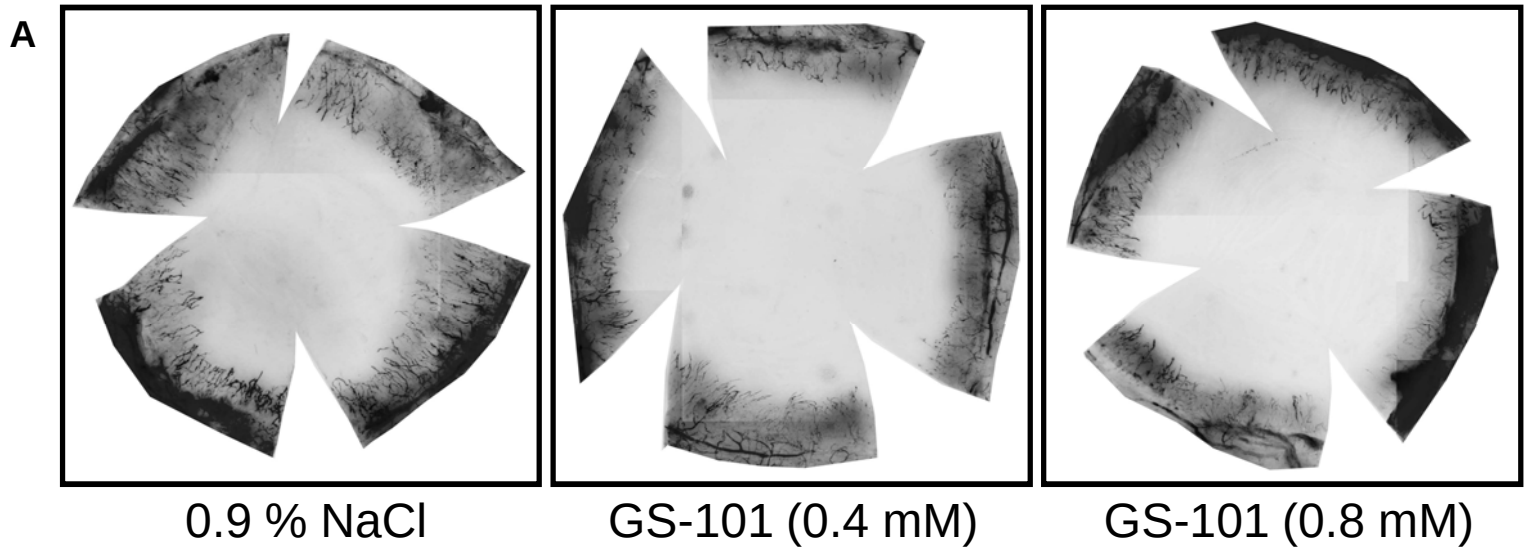

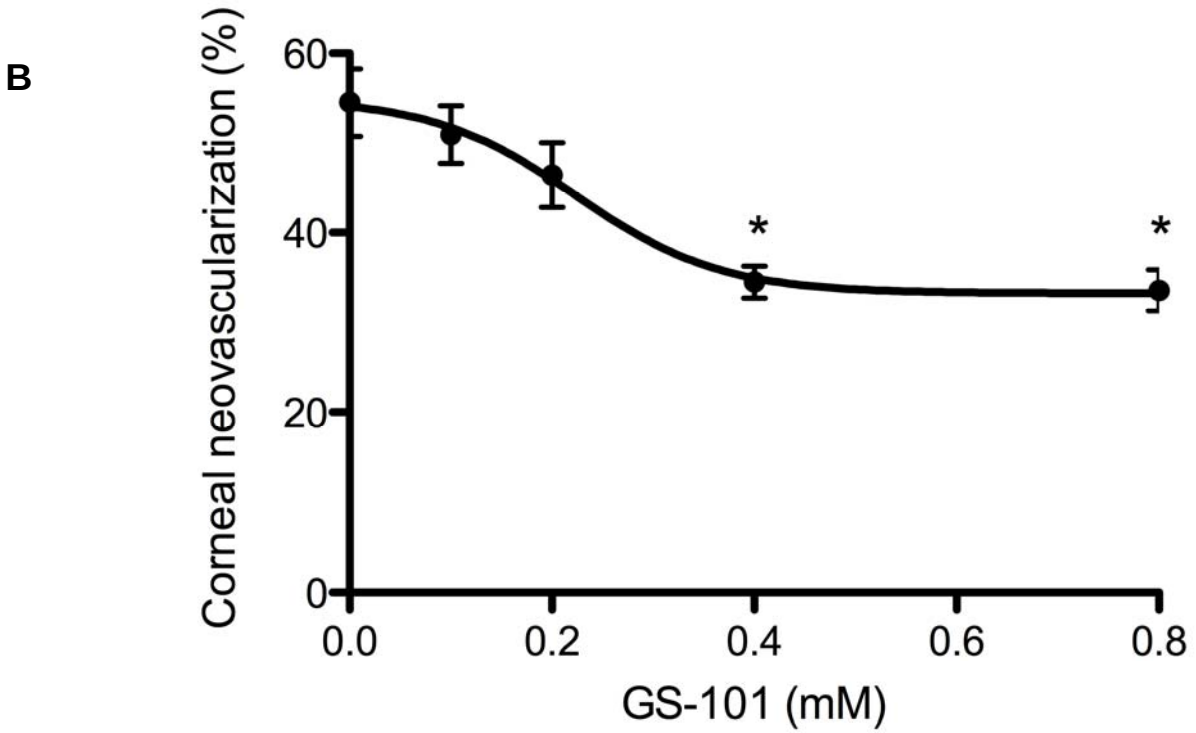

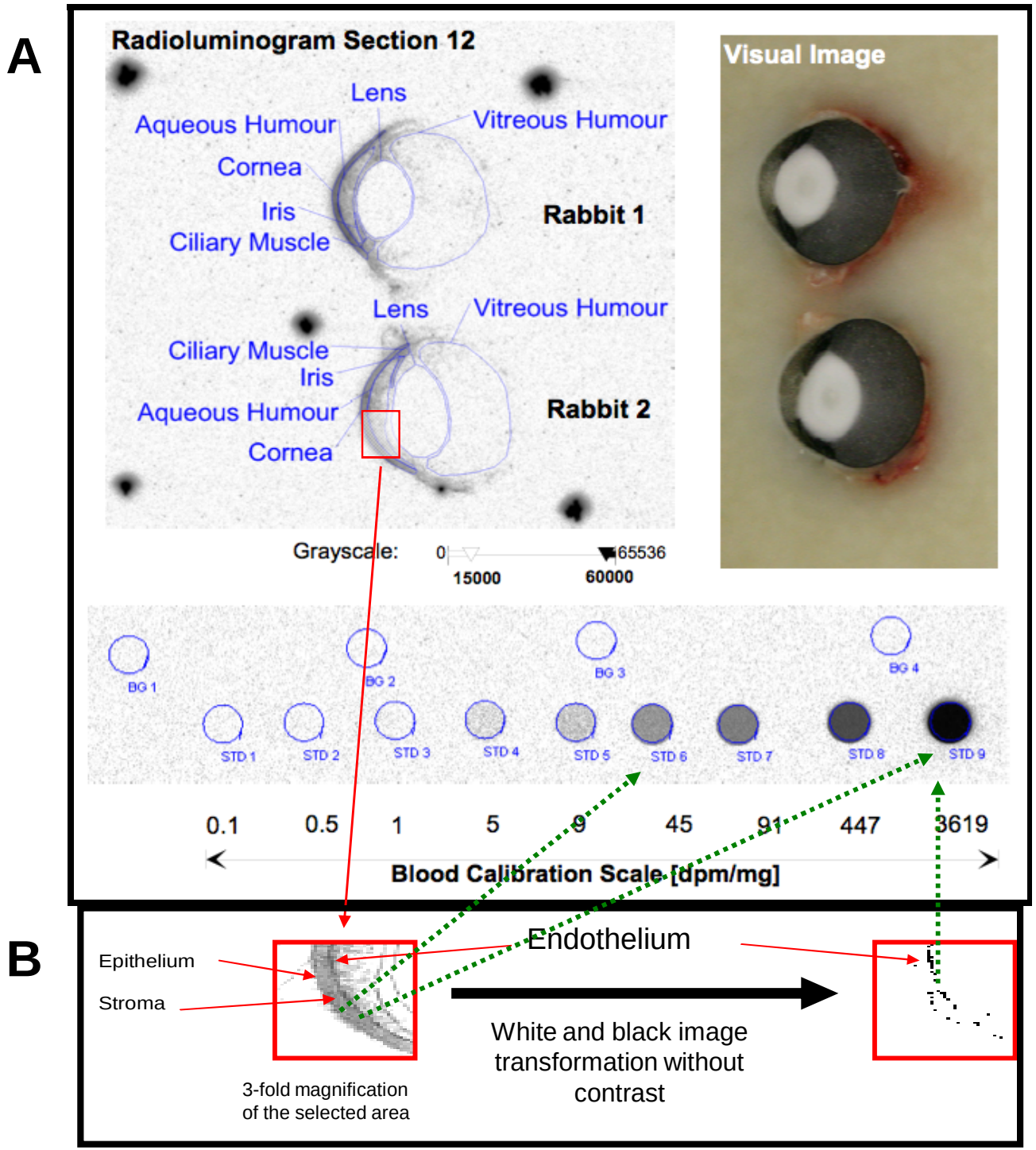

Figure 7